

Hexagonally ordered 100 nm period nickel nanowire arrays

K. Nielsch,^{a)} R. B. Wehrspohn, J. Barthel, J. Kirschner, and U. Gösele
Max-Planck-Institute of Microstructure Physics, Weinberg 2, 06120 Halle, Germany

S. F. Fischer and H. Kronmüller
Max-Planck-Institute of Metal Research, Heisenbergstrasse 1, 70569 Stuttgart, Germany

(Received 9 November 2000; accepted for publication 6 July 2001)

The magnetic behavior of 100 nm period arrays of Ni nanowires embedded in a highly ordered alumina pore matrix were characterized by magnetometry and magnetic force microscopy. Reducing the diameter of the nanowires from 55 to 30 nm while keeping the interwire distance constant leads to increasing coercive fields from 600 to 1200 Oe and to increasing remanence from 30% to 100%. The domain structure of the arrays exhibits in the demagnetized state a labyrinth-like pattern. These results show that stray field interactions of single domain nanowires are entirely dependent on the nanowire diameter. © 2001 American Institute of Physics. [DOI: 10.1063/1.1399006]

Since 1991, the increase in storage density for commercially available hard disks has been 60% per year. Nowadays, hard disks with an areal density of about 10 Gbit/in.² are commercially available, and a number of companies have demonstrated densities ranging up to 50 Gbit/in.² in their laboratories. If the increase in areal density continues, the predicted superparamagnetic limit of about 70 Gbit/in.² might be reached for products in a few years.¹ One approach to extend this limit is via patterned perpendicular media,^{2–5} in which one bit of information corresponds to one single domain nanosized particle, a so-called nanomagnet. Since each bit would be composed of a single high-aspect particle, the areal density of these patterned media can, in principle, be much more than one order of magnitude higher than in conventional longitudinal media. For example, an areal density of about 300 Gbit/in.² can be achieved by a hexagonally arranged array of nanomagnets with a lattice constant of about 50 nm.

One promising technique with which to obtain nanomagnet arrays is based on hexagonally arranged porous alumina templates.^{6–12} Since 1981 there have been numerous publications about ferromagnetic-material-filled unarranged porous alumina templates.^{6–11} These structures have large pore diameter size distributions and interpore distances and the degree of filling of the pores is not specified. Based on an approach by Masuda and Fukuda,¹³ we have shown that ordered porous alumina arrays with a sharply defined pore diameter can be obtained by a two-step electrochemical anodization aluminum process.^{14,15} The degree of self-ordering is polydomain with a typical domain size of a few microns. The interpore distance ($D_{\text{int}}=50\text{--}500\text{ nm}$), the pore diameter ($0.3 \times D_{\text{int}} < D_p < D_{\text{int}}$) and the length ($0.2\text{--}200\ \mu\text{m}$) can be varied over a wide range.^{13–15} Using pulsed electrodeposition, we homogeneously filled Ni and Co into porous alumina templates¹² (Fig. 1). Ferromagnetic nanowires (light) are embedded into the porous alumina matrix (dark). Nearly 100% pore filling was obtained for all samples.¹² The nanowires consist of nanocrystallites of between 20 and 100 nm which have a mostly tetrahedral shape, a face-centered-

cubic (fcc) lattice, and preferential $\langle 110 \rangle$ orientation perpendicular to the nanowire axis as determined by high-resolution transmission electron microscopy.

The field dependent magnetization hysteresis was measured for three Ni-filled samples at room temperature by a superconducting quantum interference device (SQUID) magnetometer. Figure 2 shows the hysteresis loops of hexagonally ordered Ni nanowire arrays with a pitch of 100 nm, a nanowire length of 1 μm , and pore diameters of about $D_p=55\text{ nm}$ (sample A), 40 nm (sample B), and 30 nm (sample C). The external field was applied parallel (\parallel) and perpendicular (\perp) to the long axes of the nanowires. The hysteresis for sample A measured in the \parallel direction shows a coercive field of $H_C^{\parallel} \approx 600\text{ Oe}$ and squareness of about 30% [Fig. 2(a)]. For the \perp direction the hysteresis shows a low coercive field of $H_C^{\perp} \approx 100\text{ Oe}$. The hysteresis for both directions exhibits similar saturation fields ($H_S^{\parallel} \approx 4000\text{ Oe}$). Therefore, this sample does not have a preferential magnetic orientation. In contrast, sample B exhibits increased coercive fields of about $H_C^{\parallel} = 1000\text{ Oe}$ and improved magnetic hardness ($\approx 80\%$ squareness). This sample has a preferential magnetic orientation along the wire axis ($H_S^{\parallel} \approx 3200$, $H_S^{\perp} \approx 5500\text{ Oe}$, and $H_C^{\parallel} \gg H_C^{\perp}$). With sample C ($D_p=30\text{ nm}$) squareness of 98% and the highest coercive field $H_C^{\parallel} = 1200\text{ Oe}$ [Fig. 2(c)], which is the highest reported coercivity for a high-density

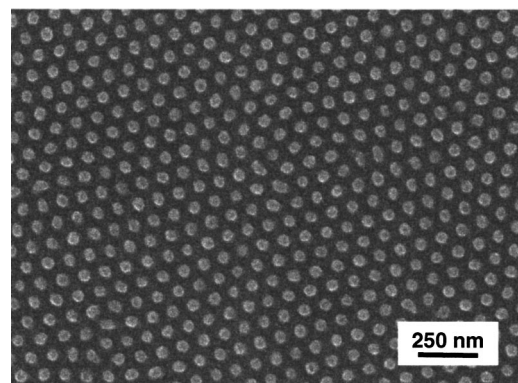


FIG. 1. Top-view scanning electron micrograph of a Ni-filled alumina membrane (sample B) with a pitch of 100 nm and $D_p \approx 40\text{ nm}$.

^{a)}Electronic mail: elch@mpi-halle.de

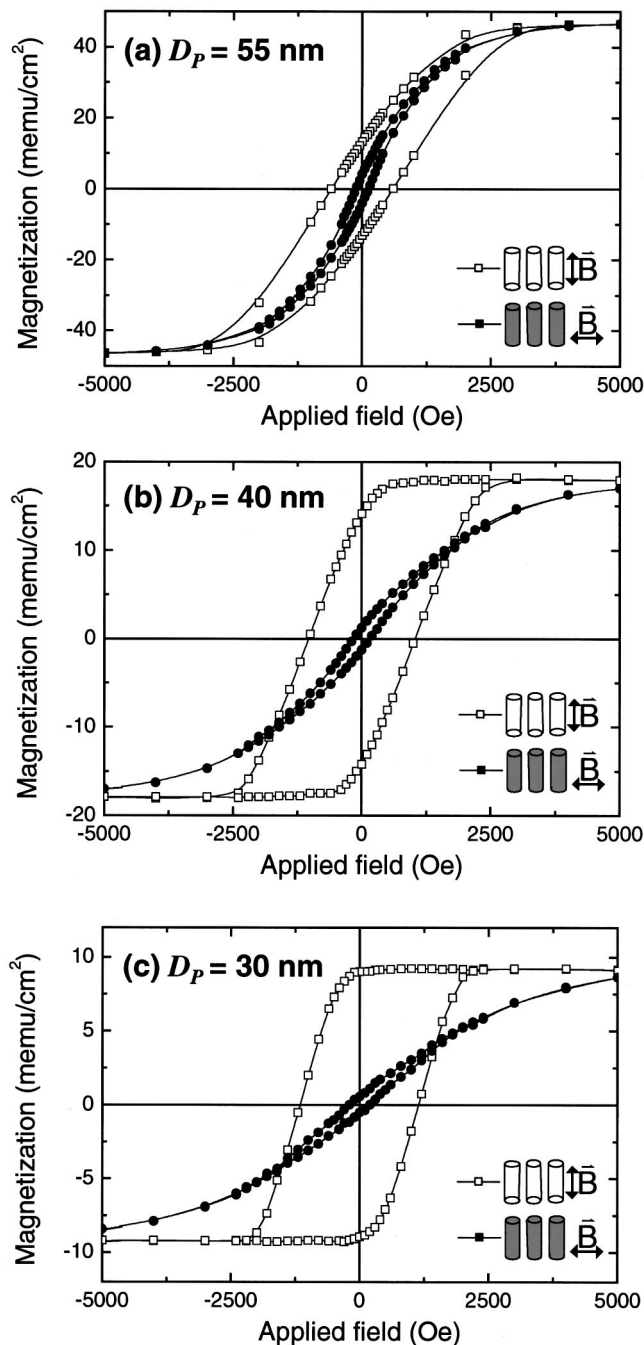


FIG. 2. SQUID hysteresis loops for hexagonally ordered Ni nanowire arrays with a pitch of 100 nm and pore diameters of $D_p \approx 55$ (a), ≈ 40 (b), and ≈ 30 nm (c).

($D_{int} \leq 100$ nm) Ni nanowire array,^{3-6,11} were obtained. Samples B and C have a similar magnetic anisotropy. In the following, the bulk value of the saturation magnetization $M_s = 484$ emu/cm³ is used. By determining the absolute amount of nickel in the pores by atom absorption spectroscopy and relating it to the absolute magnetization by SQUID magnetometry, we obtain $M_s = 480 \pm 25$ emu/cm³.

The magnetic anisotropy of an array of thin magnetic wires results from the interplay of a series of effective fields. In the case of a single domain wire, which is expected for Ni with diameters smaller than 55 nm,¹⁶ we have to consider three contributions: (1) the macroscopic demagnetization field due to the average magnetic charges of the wires at the surface. For Ni and the geometry of the hexagonal pore

structure the average derived demagnetization field ($-4\pi M_s P$; $P \approx$ porosity of the template structure) is about -1750 Oe for 55 nm pores, -920 Oe for 40 nm pores, and -520 Oe for 30 nm pores. (2) The form effect of the individual wire if magnetized parallel to the pore axis is of the order of $2\pi M_s = 3200$ Oe. (3) A third contribution results from the magnetocrystalline anisotropy energy, given by $(-4K_1/3M_s) \approx 120$ Oe for Ni with K_1 the magnetocrystalline anisotropy.

Reducing the pore diameter from 55 to 30 nm while keeping the interpore distance constant, the remanence increases up to nearly 100% and the coercive field shifts towards 1200 Oe. Sample B with $D_p = 40$ nm and sample C with $D_p = 30$ nm are single domain wires, which are preferentially magnetized in the \parallel -direction because the form effect of 3200 Oe easily overcomes the crystal field of 120 Oe. The theoretical effective coercive field of a single infinitely extended cylinder magnetized parallel to the $\langle 111 \rangle$ easy direction of the Ni cylinder axis for homogeneous rotation is given by $H_c^{\parallel} = 4K_1/3M_s + 2\pi M_s$. This holds if the cylinder diameter is smaller than the critical diameter D_{crit} for the curling process,¹⁷ $D_p \leq D_{crit} = 3.68\sqrt{A/\pi M_s^2}$ ($A = 8.6 \times 10^{-7}$ erg/cm for Ni) yielding for Ni $D_{crit} = 40$ nm. Therefore, the curling mode is not an appropriate description for the magnetization of samples B and C. In addition, the demagnetizing field, $4\pi M_s P$, of the arrays has to be taken into account. By neglecting the magnetocrystalline anisotropy, one obtains $H_c^{\parallel} = 2\pi M_s(1-2P)$ which is for $D_p = 40$ nm $\rightarrow H_c^{\parallel} = 2100$ Oe and for $D_p = 30$ nm $\rightarrow H_c^{\parallel} = 2500$ Oe. The measured smaller coercive fields of ≈ 1000 and ≈ 1200 Oe indicate that the Stoner-Wohlfarth approximation of the switching fields is not valid. Holz^{18,19} showed that at the wire ends a butterfly-type arrangement of magnetization exists which reduces the switching field considerably. Recently, it was shown by computer simulation^{20,21} that for an aspect ratio of 20:1 and $D_p \approx 40$ nm the nucleation field is reduced by about a factor of 2 which agrees rather well with the results for the 40 nm wires. Experimental results obtained for isolated wires also agree reasonably well with the computer simulation.²² In the case of an array of nanowires, in addition, collective demagnetization modes have to be taken into account which leads to a further decrease of the switching field.²³ The micromagnetic modeling reported by Hertel²³ results in coercive fields of 1400 Oe for a single Ni wire and about 1100 Oe and remanence of 100% for a hexagonal 100 nm period Ni wire array composed of 16 nanowires with diameters of about 40 nm. These values are in good agreement with our data.²³

The observed squareness of less than 100% for sample B might result from imperfections of the polydomain pore array. The demagnetization field can locally overcome the switching field of an individual magnetic wire. These single nanomagnets will reverse their magnetic polarization to achieve a lower energetic state and to reduce their demagnetization field. This is observed for $D_p = 40$ nm (sample B), where approximately 10% of the nickel columns switch their magnetic polarization into the opposite direction after the whole sample has been magnetized along the wire axis when the applied field is zero.

In contrast, the same templates filled with cobalt exhibit

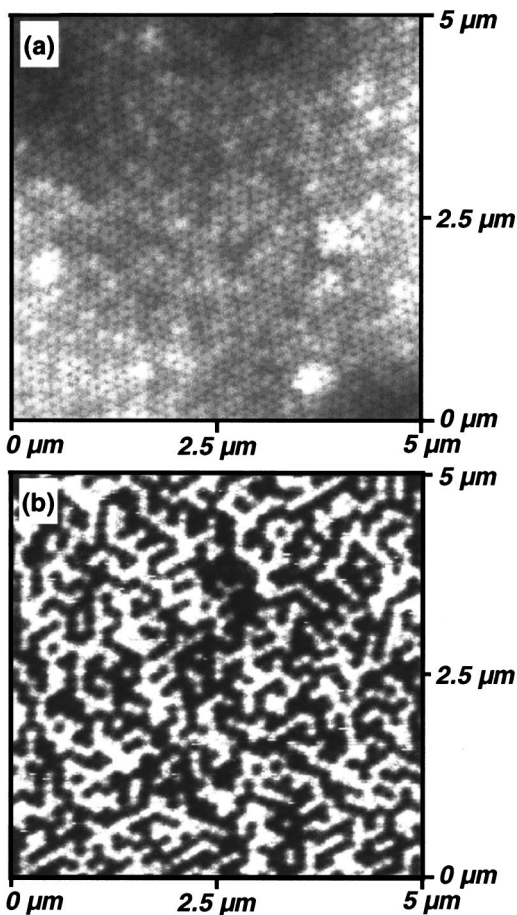


FIG. 3. Topographic image of a highly ordered alumina template with a pitch of 100 nm filled with $D_p \approx 40$ nm Ni nanowires (a). The corresponding MFM image (b) of the sample in the demagnetized state, showing the pillars magnetized alternately "upward" (light) and "downward" (dark).

low coercive fields ($H_C^{\parallel} < 500$ Oe) and high saturation fields ($H_S^{\parallel} > 5000$ Oe).²⁴ Like Metzger *et al.*,²⁵ we observe a strong interaction between the nanowires and a preferential magnetocrystalline anisotropy perpendicular to the wire axis. As long as the crystalline orientation cannot be controlled, Co is not a suitable candidate for perpendicular storage media, in line with Ref. 25.

A magnetic force microscopy (MFM) image of sample B in the demagnetized state and the corresponding topography are shown in Fig. 3. Dark spots in Fig. 3(b) indicate magnetization pointing upward and bright spots indicate magnetization pointing downward. Upward magnetization may be interpreted as the binary "1" and downward magnetization as the binary "0." It can be deduced from the image that the Ni pillars are single domain nanomagnets aligned perpendicular to the surface. The patterned domain structure is due to antiferromagnetic alignment of the pillars influenced by the weak magnetic interaction between these nanomagnets. The labyrinth pattern [Fig. 3(b)] of the domain structure is characteristic of a hexagonally arranged single domain magnetic particle with perpendicular magnetic orientation in the demagnetized state. In the case of a quadratic lattice, each of the four nearest neighbors will be aligned antiparallel and the domain structure exhibits a checkerboard pattern.⁵ In the hexagonal lattice, two of the six nearest neighbors will align

their magnetization parallel and four will be magnetized antiparallel if the stray field has only nearest neighbor interaction. In Fig. 3, we observe that, on average, 2.5 nanomagnets are aligned parallel and 3.5 are magnetized antiparallel. We suppose that stray field interaction is extended over several interpoles due to the high aspect ratio of the magnetic nanowires.

In conclusion, the bulk magnetic properties of Ni nanowires arranged in a hexagonal pattern with a pitch of 100 nm were studied by SQUID magnetometry. Reducing the diameter of magnetic columns from $D_p = 55$ to 30 nm improves the hardness of the magnetic hysteresis and raises the coercivity from 600 up to 1200 Oe. This is due to a reduction in macroscopic interactions between the nanomagnets and enhancement of the switching field of the individual nanowire. The domain structure of highly ordered arrays of Ni columns is labyrinth like. Each magnetic pillar is a single domain magnetic particle, magnetized perpendicular to the template surface. Due to the fact that 100% squareness and low stray field interactions were detected for the sample with $D_p \approx 30$ nm, we expect that for this sample each Ni nanowire is able to be switched independently to the magnetization of its nearest neighbors and store one bit of information.

The authors would like to thank Dr. R. Hertel for fruitful discussions concerning magnetic modeling.

- ¹D. Weller and A. Moser, IEEE Trans. Magn. **35**, 4423 (1999).
- ²R. O'Barr, S. Y. Yamamoto, S. Schultz, W. Xu, and A. Scherer, J. Appl. Phys. **81**, 4730 (1997).
- ³S. Y. Chou, M. S. Wei, P. R. Krauss, and P. B. Fischer, J. Appl. Phys. **76**, 6673 (1994).
- ⁴C. A. Ross, H. I. Smith, T. A. Savas, M. Schattenberg, M. Farhoud, M. Hwang, M. Walsh, M. C. Abraham, and R. J. Ram, J. Vac. Sci. Technol. B **17**, 3168 (1999).
- ⁵M. Hwang, M. C. Abraham, T. A. Savas, H. I. Smith, R. J. Ram, and C. A. Ross, J. Appl. Phys. **87**, 5108 (2000).
- ⁶M. P. Kaneko, IEEE Trans. Magn. **MAG-17**, 1468 (1981).
- ⁷M. Shiraki, Y. Wakui, T. Tokushima, and N. Tsuya, IEEE Trans. Magn. **MAG-21**, 1465 (1985).
- ⁸D. AlMawlawi, N. Coombs, and M. Moskovits, J. Appl. Phys. **69**, 5150 (1991).
- ⁹L. Feiyue, R. M. Metzger, and W. D. Doyle, IEEE Trans. Magn. **33**, 3715 (1997).
- ¹⁰G. J. Strijkers, J. H. J. Dalderop, M. A. A. Broeksteeg, H. J. M. Swagten, and W. J. M. de Jonge, J. Appl. Phys. **86**, 5141 (1999).
- ¹¹H. Zeng, M. Zheng, R. Skomski, D. J. Sellmyer, Y. Liu, L. Menon, and S. Bandyopadhyay, J. Appl. Phys. **87**, 4718 (2000).
- ¹²K. Nielsch, F. Müller, A. P. Li, and U. Gösele, Adv. Mater. **12**, 582 (2000).
- ¹³H. Masuda and K. Fukuda, Science **268**, 1466 (1995).
- ¹⁴A. P. Li, F. Müller, A. Birner, K. Nielsch, and U. Gösele, J. Appl. Phys. **84**, 6023 (1998).
- ¹⁵A. P. Li, F. Müller, and U. Gösele, Electrochem. Soc. Lett. **3**, 131 (2000).
- ¹⁶*Supermagnets, Hardmagnetic Materials*, edited by G. J. Long and F. Grandjean (Kluwer Academic, Dordrecht, 1991), pp. 461–498.
- ¹⁷A. Aharoni and S. Shtrikman, Phys. Rev. **109**, 1522 (1958).
- ¹⁸A. Holz, Z. Angew. Phys. **23**, 170 (1967).
- ¹⁹A. Holz, Phys. Status Solidi **26**, 751 (1968).
- ²⁰C. Seberino and H. N. Bertram, IEEE Trans. Magn. **33**, 3055 (1997).
- ²¹H. Suhl and H. N. Bertram, J. Appl. Phys. **82**, 6128 (1997).
- ²²R. O'Barr and S. Schultz, MMM'96, Atlanta, 1996.
- ²³R. Hertel, J. Magn. Magn. Mater. (in press).
- ²⁴K. Nielsch, F. Müller, R. B. Wehrspohn, U. Gösele, S. F. Fischer, and H. Kronmüller, *Proceedings of the Electrochemical Society*, Series PV 2000-8 (The Electrochemical Society, Pennington, NJ, 2000).
- ²⁵R. M. Metzger, V. V. Konovalov, M. Sun, T. Xu, G. Zangari, B. Xu, M. Benakli, and W. D. Doyle, IEEE Trans. Magn. **36**, 30 (2000).